

ORIENTATION-REVERSING INVOLUTIONS OF THE GENUS 3 ARNOUX–YOCOZ SURFACE AND RELATED SURFACES

JOSHUA P. BOWMAN

ABSTRACT. We present a new description of the genus 3 Arnoux–Yoccoz translation surface in terms of its Delaunay polygons and show that, up to affine equivalence, it belongs to two families of surfaces whose isometry groups include the dihedral group of the square.

1. INTRODUCTION

1.1. **Flat surfaces.** For our purposes, a *flat surface* is a pair (X, q) , where X is a Riemann surface and q is a non-zero meromorphic quadratic differential of finite area on X . We will also speak of the flat surface (X, ω) instead of (X, ω^2) when $q = \omega^2$ is the global square of an abelian differential ω ; in this case, (X, ω) is also called a *translation surface*. A quadratic differential determines a canonical metric structure on the underlying surface (cf. [HM, EG]); we will consider two flat surfaces to be the same when there is an isometry between them.

Recall that $\mathrm{SL}_2(\mathbb{R})$ and $\mathrm{GL}_2(\mathbb{R})$ act on the space of translation surfaces, while $\mathrm{PSL}_2(\mathbb{R})$ and $\mathrm{PGL}_2(\mathbb{R})$ act on the space of flat surfaces. If $A \cdot (X, \omega) = (X, \omega)$ or $[A] \cdot (X, q) = (X, q)$, then $\det A = \pm 1$. The set of all $[A] \in \mathrm{PGL}_2(\mathbb{R})$ such that $[A] \cdot (X, q) = (X, q)$ form the *projective generalized Veech group* of (X, q) , which we will simply call the Veech group (cf. [Ve1, HS]).

The results in this article began with a study of Delaunay polygons on the surface described in §1.2, and so we recall their definition (cf. [MS, Ri, Ve2, BS]). A *Delaunay triangle* on (X, q) is the image of a 2-simplex on X , embedded on its interior, whose vertices lie in the set of cone points of q , whose edges are geodesic with respect to the metric of q , and whose (possibly immersed) circumcircle contains no cone points of q in its interior. A *Delaunay triangulation* of (X, q) is a cell structure on X whose 2-cells are Delaunay triangles. A *Delaunay polygon* is a Delaunay triangle or the union of two or more adjacent Delaunay triangles that share the same circumcircle.

A generic flat surface has a unique Delaunay triangulation. When it is not unique, we can start with any Delaunay triangulation and join two or more adjacent Delaunay triangles to form a Delaunay polygon. After forming all of the maximal Delaunay polygons from a Delaunay triangulation, we obtain the *Delaunay decomposition* of (X, q) , which is invariant under isometries of (X, q) .

1.2. **The Arnoux–Yoccoz surface.** In [AY], P. Arnoux and J.-C. Yoccoz introduced a family of pseudo-Anosov diffeomorphisms, one for each genus at least 3. Hubert–Lanneau [HL] showed that none of these surfaces has a Veech group containing any parabolic elements. The genus 3 example, also appearing in [Ar], has received much attention recently. Hubert–Lanneau–Möller [HLM] showed that the relevant abelian differential has a second,

2000 Mathematics Subject Classification: 30F30; 32G15, 05B45, 57M50, 14K20.

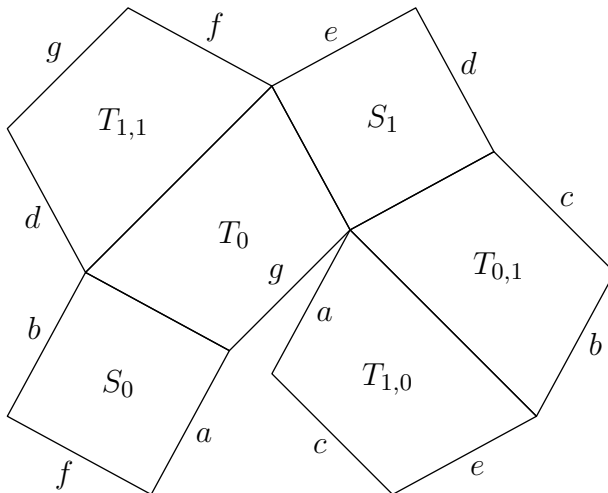


FIGURE 1. The decomposition of (X_{AY}, ω_{AY}) into its Delaunay polygons. Edges with the same label are identified by translation.

independent pseudo-Anosov element in its stabilizer, and using techniques introduced by C. McMullen [Mc] in the study of genus 2 orbits they showed that the $SL_2(\mathbb{R})$ -orbit of the genus 3 example is dense in the largest possible region of the moduli space of abelian differentials. Here we give a new description of the genus 3 surface in terms of its Delaunay polygons (of which there are only two kinds, up to isometry) and very simple gluing instructions.

Let $\alpha \approx 0.543689$ be the real root of the polynomial $x^3 + x^2 + x - 1$. Let S_0 be the square with vertex set $\{(0, 0), (\alpha^2, \alpha), (\alpha^2 - \alpha, \alpha^2 + \alpha), (-\alpha, \alpha^2)\}$, and let T_0 be the trapezoid with vertex set $\{(0, 0), (1 - \alpha, 1 - \alpha), (1 - \alpha - \alpha^2, 1), (-\alpha, \alpha^2)\}$. We form a flat surface (X_{AY}, ω_{AY}) from two copies of S_0 and four copies of T_0 : reflecting S_0 across either a horizontal or vertical axis yields the same square S_1 (up to translation); we denote by $T_{1,0}$, $T_{0,1}$, and $T_{1,1}$ the reflections of T_0 across a vertical axis, across a horizontal axis, and across both, respectively. (In fact, $T_{1,0}$, $T_{0,1}$, and $T_{1,1}$ are all rotations of T_0 by multiples of $\pi/2$, but this description via reflections will be invariant under horizontal and vertical scaling, i.e., the Teichmüller geodesic flow.) Identify the long base of T_0 with the long base of $T_{1,1}$, as well as their short bases; do the same with $T_{1,0}$ and $T_{0,1}$. Each remaining side of a trapezoid is parallel to exactly one side of S_0 or S_1 ; identify by translations those sides which are parallel. (See Figure 1.)

The resulting flat surface (X_{AY}, ω_{AY}) has genus 3 and two singularities each with cone angle 6π . The images of S_0 and T_0 are the Delaunay polygons of ω_{AY} . X_{AY} is hyperelliptic; the hyperelliptic involution $\tau : X_{AY} \rightarrow X_{AY}$ is evident in Figure 1 as rotation by π around the centers of the squares and the midpoints of the edges joining two trapezoids; these six points together with the cone points are therefore the Weierstrass points of the surface. (See Figure 3 for the quotient of X_{AY} by τ .) Moreover, ω_{AY} is odd with respect to τ , i.e., $\tau^*\omega_{AY} = -\omega_{AY}$.

The pseudo-Anosov diffeomorphism ψ_{AY} constructed by Arnoux–Yoccoz scales the surface by a factor of $1/\alpha$ in the horizontal direction and by α in the vertical direction. In Figure 2 we show the result of applying this affine map to Figure 1, along with the new Delaunay

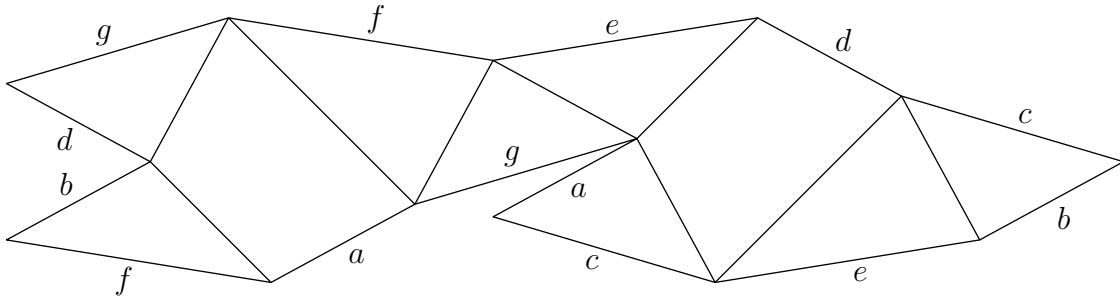


FIGURE 2. The result of applying the Arnoux–Yoccoz pseudo-Anosov diffeomorphism to ω_{AY} . The original shapes of S_0 and T_0 and their copies can be reconstructed by matching edges.

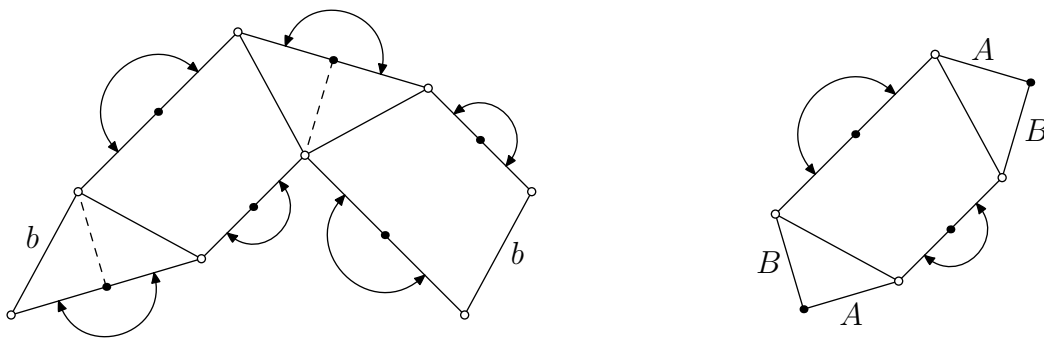


FIGURE 3. Quotient surfaces of X_{AY} . LEFT: \mathbb{CP}^1 as the quotient of X_{AY} by $\langle \tau \rangle$. The edges marked b are identified by translation. RIGHT: \mathbb{RP}^2 as the quotient of X_{AY} by the group $\langle \sigma_1, \sigma_2 \rangle$. Edges with the same label are identified by a glide reflection along either a horizontal or a vertical axis. Dashed lines in the left picture indicate preimages of the segments labeled B on the right.

edges. Two of the trapezoids—having the orientations of $T_{1,1}$ and $T_{1,0}$ —are clearly visible; the squares and the other two trapezoids are constructed from the remaining triangles.

1.3. X_{AY} as a cover of \mathbb{RP}^2 . The reflections applied to S_0 and T_0 in §1.2 induce a pair of orientation-reversing involutions without fixed points on X_{AY} . These can be visualized (as in Figure 1) as “glide-reflections”, one along a horizontal axis and the other along a vertical axis. Both exchange S_0 and S_1 . Let σ_1 be the involution that exchanges T_0 and $T_{1,0}$; i.e., its derivative is reflection across the horizontal axis. Let σ_2 be the involution that exchanges T_0 and $T_{0,1}$; i.e., its derivative is reflection across the vertical axis. The product of σ_1 and σ_2 is the hyperelliptic involution τ , and neither sends any point of X_{AY} to its image by τ . They therefore descend to a single involution σ on \mathbb{CP}^1 without fixed points. The quotient of \mathbb{CP}^1 by σ is homeomorphic to \mathbb{RP}^2 .

In fact, the presence of σ_1 and σ_2 is implicit in the work of Arnoux–Yoccoz. The original paper [AY] begins with a measured foliation of \mathbb{RP}^2 with one “tripod” (a singular point of valence three) and three “thorns” (singular points of valence 1), which is then lifted to the genus 3 example we have described. In Figure 3, right, we illustrate \mathbb{RP}^2 as the quotient of X_{AY} by the group generated by σ_1 and σ_2 . In Figure 3, left, we see \mathbb{CP}^1 , on which σ acts again by a “glide-reflection”, which is the sheet exchange for the cover $\mathbb{CP}^1 \rightarrow \mathbb{RP}^2$. In

both pictures we have drawn vertices that become tripods as open circles, and the vertices that become thorns as filled-in circles. The vertical foliation of the surface on the right of Figure 3 is the starting point of [AY].

In §2 we will show that both (X_{AY}, ω_{AY}) and another affinely equivalent surface have *real structures* (orientation-reversing involutions whose fixed-point set is 1-dimensional) that are not evident in the original construction. These additional structures will allow us to write equations for the surfaces and fit them into families of flat surfaces with a common group of isometries. In §3 we will transfer these results to genus 2 quadratic differentials. In §4 we will conclude by showing that we have found all the surfaces that are obtained by applying the geodesic flow to (X_{AY}, ω_{AY}) and have real structures.

2. TWO FAMILIES OF SURFACES

2.1. Labeling the Weierstrass points of X_{AY} . As before, we denote the hyperelliptic involution of X_{AY} by τ , and we let σ_1 and σ_2 be the involutions described in §1.3, with $\sigma : \mathbb{CP}^1 \rightarrow \mathbb{CP}^1$ the involution covered by both σ_1 and σ_2 .

The purpose of this section is to show the following.

Theorem 2.1. *The surface (X_{AY}, ω_{AY}) belongs to a family $(X_{t,u}, \omega_{t,u})$, with $t > 1$ and $u > 0$, such that $X_{t,u}$ has the equation*

$$(1) \quad y^2 = x(x-1)(x-t)(x+u)(x+tu)(x^2+tu),$$

and $\omega_{t,u}$ is a multiple of $x dx/y$ on $X_{t,u}$.

Each of the surfaces in Theorem 2.1 has a pair of real structures ρ_1 and ρ_2 whose product is again τ , and which therefore descend to a single real structure ρ on \mathbb{CP}^1 . Any product of the form $\rho_i \sigma_j$ ($i, j \in \{1, 2\}$) is a square root of τ , and therefore the group generated by $\{\sigma_1, \sigma_2, \rho_1, \rho_2\}$ is the dihedral group of the square. We will exhibit these isometries in our presentation of (X_{AY}, ω_{AY}) . In §2.3 we will look at surfaces in this family that have additional symmetries.

Let $\varpi : X_{AY} \rightarrow \mathbb{CP}^1$ be the degree 2 map induced by τ , i.e., $\varpi \circ \tau = \varpi$. We can normalize ϖ so that the zeroes of ω_{AY} are sent to 0 and ∞ , and the midpoint of the short edge between T_0 and $T_{1,1}$ is sent to 1. We wish to find the images of the remaining Weierstrass points, so that we can write an affine equation for X_{AY} in the form $y^2 = P(x)$, where P is a degree 7 polynomial with roots at 0 and 1. Hereafter we assume that ϖ is the restriction to X_{AY} of the coordinate projection $(x, y) \mapsto x$. Consequently, we may consider each Weierstrass point as either a point $(w, 0)$ that solves $y^2 = P(x)$ or simply as a point w on the x -axis.

Each of the real structures ρ_1 and ρ_2 has a fixed-point set with three components: in one case, say ρ_1 , the real components are the line of symmetry shared by T_0 and $T_{1,1}$, and the two bases of $T_{1,0}$ and $T_{0,1}$. The fixed-point set of ρ_2 is then the union of the corresponding lines in the orthogonal direction. Because ρ_1 and ρ_2 fix the points 0, 1, and ∞ , ρ fixes the real axis; therefore ρ is simply complex conjugation.

With this normalization, the involution σ on \mathbb{CP}^1 exchanges 0 and ∞ and preserves the real axis; therefore σ has the form $x \mapsto -r/\bar{x}$ for some real $r > 0$.

Let $s = (s, 0)$ be the center of S_0 . Then $\rho_1(s) = \rho_2(s) = \sigma_1(s) = \sigma_2(s)$ is the center of S_1 , which implies $\rho(s) = \sigma(s)$, i.e., $\bar{s} = -r/\bar{s}$. The solutions to this equation are $\pm i\sqrt{r}$. By considering the location of the fixed-point sets of ρ_1 and ρ_2 , we see that the image of S_0 by ϖ lies in the upper half-plane; therefore $s = i\sqrt{r}$, and $-i\sqrt{r}$ is the center of S_1 .

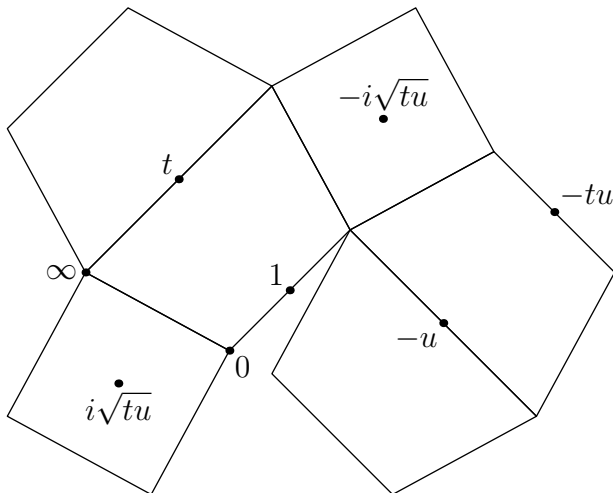


FIGURE 4. The Weierstrass points of X_{AY} , following normalization ($t > 1$, $u > 0$). The real structures ρ_1 and ρ_2 appear as reflections in the lines of slope ± 1 .

Let t be the midpoint of the long edge of T_0 . Applying σ_1 or σ_2 shows that the midpoint of the long edge of $T_{1,0}$ is at $-r/t$.

We already know that 1 is the center of the short edge of T_0 . Since the short edge of $T_{0,1}$ is the image of this edge by σ_1 or σ_2 , the midpoint of this edge must be at $-r$.

To simplify notation, let us make the substitution $u = r/t$, so that $r = tu$ (hence σ has the form $\sigma(x) = -tu/\bar{x}$). Thus X_{AY} has the equation (1) for some $(t, u) = (t_{AY}, u_{AY})$. Furthermore, ω_{AY} is the square root of a quadratic differential on \mathbb{CP}^1 with simple zeroes at 0 and ∞ and simple poles at 1, t , $-u$, $-tu$, and $\pm i\sqrt{tu}$. There is therefore some complex constant c such that

$$\omega_{AY}^2 = \varpi^* \left(\frac{cx}{(x-1)(x-t)(x+u)(x+tu)(x^2+tu)} dx^2 \right),$$

i.e., $\omega_{AY} = \pm\sqrt{c}x dx/y$. This establishes Theorem 2.1.

2.2. Integral equations. To find t_{AY} and u_{AY} requires solving a system of equations involving hyperelliptic integrals, which we establish in this section using relative periods of ω_{AY} . Choose a square root of

$$f_{t,u}(x) = \frac{x}{(x-1)(x-t)(x+u)(x+tu)(x^2+tu)}$$

in the open first quadrant such that its extension $\sqrt{f_{t,u}(x)}$ to the complement of $\{1, t, i\sqrt{tu}\}$ in the closed first quadrant is positive on the open interval $(0, 1)$. Let η_0 be the Delaunay edge between S_0 and T_0 ; $\varpi(\eta_0)$ is then a curve from 0 to ∞ in the first quadrant. Integrating $\sqrt{cf_{t,u}(x)} dx$ on the portion of the first quadrant below $\varpi(\eta_0)$ will then give a conformal map to half of T_0 . We will be interested in integrals along the real axis.

The vector from 0 to 1 along the short side of T_0 is $\frac{1}{2}(1-\alpha)(1+i)$, while the the line of symmetry of T_0 from 1 to t gives the vector $\frac{1}{2}(\alpha+\alpha^2)(-1+i)$. Observe that

$$i \cdot (1-\alpha)(1+i) = \alpha \cdot (\alpha+\alpha^2)(-1+i),$$

and therefore

$$(2) \quad i \int_0^1 \sqrt{cf_{t,u}(x)} \, dx = \alpha \int_1^t \sqrt{cf_{t,u}(x)} \, dx.$$

Similarly, the vector from t to ∞ along the long side of T_0 is $\frac{1}{2}(1 - \alpha^2)(-1 - i)$, and because $1 - \alpha^2 = (1 + \alpha)(1 - \alpha)$, we have

$$(3) \quad -(1 + \alpha) \int_0^1 \sqrt{cf_{t,u}(x)} \, dx = \int_t^\infty \sqrt{cf_{t,u}(x)} \, dx.$$

In both equations we can cancel out the c , which was ever only a global (complex) scaling factor anyway. Now bring i under the square root on the right-hand side of (2) in order to make the radicand positive. We thus obtain from (2) and (3) the system of (real) integral equations

$$(4) \quad \begin{cases} \int_0^1 \sqrt{f_{t,u}(x)} \, dx = \alpha \int_1^t \sqrt{-f_{t,u}(x)} \, dx \\ (1 + \alpha) \int_0^1 \sqrt{f_{t,u}(x)} \, dx = - \int_t^\infty \sqrt{f_{t,u}(x)} \, dx \end{cases}$$

whose solution is the desired pair $(t_{\text{AY}}, u_{\text{AY}})$. Using numeric methods, we find

$$t_{\text{AY}} \approx 1.91709843377 \quad \text{and} \quad u_{\text{AY}} \approx 2.07067976690.$$

We conjecture that t_{AY} and u_{AY} lie in some field of small degree over $\mathbb{Q}(\alpha)$.

2.3. Other exceptional surfaces in this family. An examination of the geometric arguments in §2.1 and an application of the principle of continuity to t and u show the following:

Theorem 2.2. *Every $(X_{t,u}, \omega_{t,u})$ as in Theorem 2.1 can be formed by replacing T_0 in the description from §1.2 with an isosceles trapezoid T , S_0 with the square built on a leg of T , and the copies of T_0 with the rotations of T by $\pi/2$.*

The placement of t and u on \mathbb{R} determines the shape of the trapezoid T , and any isosceles trapezoid may be obtained by an appropriate choice of t and u . In this section, we examine certain shapes that give $(X_{t,u}, \omega_{t,u})$ extra symmetries and determine the corresponding values of t and u . We continue to use τ to denote the hyperelliptic involution of $X_{t,u}$.

Suppose that T is a rectangle. Then there are two orthogonal closed trajectories, running parallel to the sides of T and connecting the centers $\pm i\sqrt{tu}$ of the squares, and either of these can be made into the fixed-point set of a real structure on $X_{t,u}$. The product of these two real structures is again τ , so they descend to a single real structure on \mathbb{CP}^1 . This real structure exchanges 0 with ∞ and fixes $\pm i\sqrt{tu}$, so it must be inversion in the circle $|x|^2 = tu$. It also exchanges 1 with t , which implies $1 \cdot t = tu$, i.e., $u = 1$. The remaining parameter t is determined by solving the single integral equation

$$\int_0^1 \sqrt{\frac{x}{(x^2 - 1)(x^2 - t^2)(x^2 + t)}} \, dx = \mu \int_1^t \sqrt{\frac{-x}{(x^2 - 1)(x^2 - t^2)(x^2 + t)}} \, dx$$

where 2μ is the ratio of the width of T to its height. Recall that an *origami*, also called a *square-tiled surface*, is a flat surface that covers the square torus with at most one branch point (cf. [Sch, EO, Zo]). By looking at rational values of μ , we have the following result:

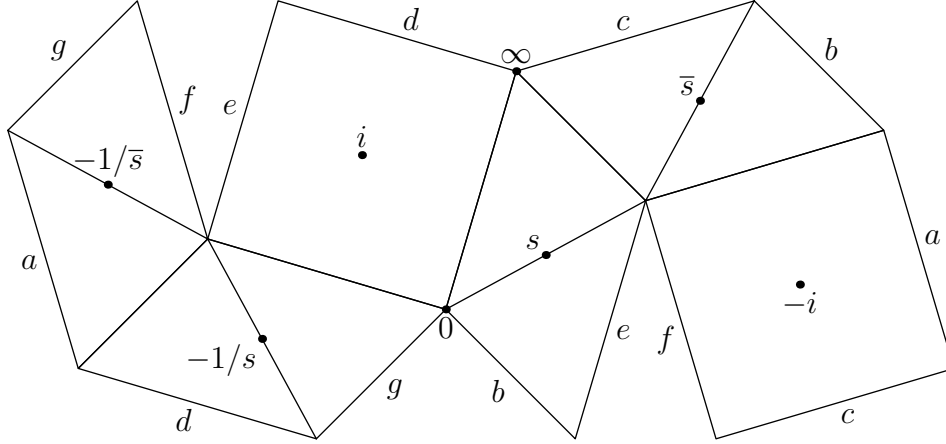


FIGURE 5. Another surface in the $\mathrm{GL}_2(\mathbb{R})$ -orbit of ω_{AY} with additional real structures. Edges with the same label are identified.

Corollary 2.3. *The family $(X_{t,1}, \omega_{t,1})$ contains a dense set of origamis.*

These are not the only $(X_{t,u}, \omega_{t,u})$ that are origamis, however. If T is a trapezoid whose legs are orthogonal to each other, then $(X_{t,u}, \omega_{t,u})$ is again an origami.

2.4. Second family of surfaces. Conjugating ρ_1 by the pseudo-Anosov element ψ_{AY} guarantees the existence of another orientation-reversing involution in the affine group of ω_{AY} . This element fixes a point “half-way” (in the Teichmüller metric, for instance) between ω_{AY} and its image by ψ_{AY} , lying in the Teichmüller disk of $(X_{\mathrm{AY}}, \omega_{\mathrm{AY}})$. This surface can be found either by scaling the vertical direction by $\sqrt{\alpha}$ and the horizontal direction by $1/\sqrt{\alpha}$ or, to keep our coordinates in the field $\mathbb{Q}(\alpha)$, just by scaling the horizontal by $1/\alpha$. This surface, which we will denote $(X'_{\mathrm{AY}}, \omega'_{\mathrm{AY}})$, is shown in Figure 5, along with its Delaunay polygons.

Theorem 2.4. *The surface $(X'_{\mathrm{AY}}, \omega'_{\mathrm{AY}})$ belongs to a family (X_s, ω_s) , with $\mathrm{Im} s > 0$ and $s \neq i$, such that X_s has the equation*

$$(5) \quad y^2 = x(x^2 + 1)(x - s)(x - \bar{s})(x + 1/s)(x + 1/\bar{s}),$$

and ω_s is a multiple of $x dx/y$ on X_s .

Again, we have two real structures ρ'_1 and ρ'_2 whose product is the hyperelliptic involution τ . Each of these only has one real component, however: the union of the sides of the parallelograms running parallel to the axis of reflection. The only Weierstrass points that lie on these components are 0 and ∞ ; the remaining Weierstrass points are the centers of the squares and of the parallelograms. We again let ρ' be the induced real structure on \mathbb{CP}^1 and assume that it fixes the real axis (this we can do because we have only fixed the positions of two points on \mathbb{P}^1), so that the remaining Weierstrass points come in conjugate pairs.

The fixed-point free involutions σ_1 and σ_2 from §1.3 again preserve the union of the real loci of ρ'_1 and ρ'_2 , and therefore they descend to a fixed-point free involution σ of the form $x \mapsto -r/\bar{x}$, with r real and positive. We have one more free real parameter for normalization, so we can assume $r = 1$. This implies that the centers of the squares are at $\pm i$. Let s be the center of one of the parallelograms; then applying ρ'_1 and σ_1 shows that the remaining

Weierstrass points are \bar{s} , $1/s$, and $1/\bar{s}$. Using developing vectors again, we can find equations that define s , in a manner analogous to finding (4).

As an analogue to Theorem 2.2, we have:

Theorem 2.5. *Every (X_s, ω_s) as in Theorem 2.4 can be formed from a parallelogram P , a square built on one side of P , the rotation of P by $\pi/2$, and the images of P and its rotation by reflection across their remaining sides.*

The shape of P is determined by the value of s . If $s = \frac{1}{2}(\sqrt{3} + i)$, then P becomes a square, and we obtain one of the “escalator” surfaces in [LS]. More generally, if s is any point of the unit circle, then P is a rectangle, and inversion in the unit circle corresponds to another pair of real structures on X , which are the reflections across the axes of symmetry of P . By considering those rectangular P whose side lengths are rationally related, we have as before:

Corollary 2.6. *The family $(X_{e^{i\theta}}, \omega_{e^{i\theta}})$ (with $0 < \theta < \pi/2$) contains a dense set of origamis.*

Another origami appears when P is composed of a pair of right isosceles triangles so that s lies not on the hypotenuse, but on a leg of each.

3. QUADRATIC DIFFERENTIALS AND PERIODS ON GENUS 2 SURFACES

We do not know how to compute the rest of the periods for $X_{t,u}$ or X_s , apart from those of $\omega_{t,u}$ or ω_s , respectively. In this section, however, we consider the periods of certain related genus 2 surfaces, which demonstrate remarkable relations.

Let X be any hyperelliptic genus 3 surface with an abelian differential ω that is odd with respect to the hyperelliptic involution and has two double zeroes. The pair (X, ω) has a corresponding pair (Ξ, q) , where Ξ is a genus 2 surface and q is a quadratic differential on Ξ with four simple zeroes. Geometrically, the correspondence may be described as follows: two of the zeroes of ω are at Weierstrass points of X , hence (X, ω^2) covers a flat surface $(\mathbb{CP}^1, \tilde{q})$ where \tilde{q} has six poles and two simple zeroes (Figure 3). Then (Ξ, q) is the double cover of $(\mathbb{CP}^1, \tilde{q})$ branched at the poles of \tilde{q} . In our cases, the genus 2 surface may be obtained by cutting along opposite sides of one of the squares in Figure 1 or 5, then regluing each of these via a rotation by π to the free edge provided by cutting along the other (cf. [La, Va]).

First we consider the family $(X_{t,u}, \omega_{t,u})$ and the related genus 2 flat surfaces $(\Xi_{t,u}, q_{t,u})$. To be explicit, the defining expressions of both types of surfaces are:

$$\begin{aligned} X_{t,u} : y^2 &= x(x-1)(x-t)(x+u)(x+tu)(x^2+tu), & \omega_{t,u} &= \frac{x dx}{y}; \\ \Xi_{t,u} : y^2 &= (x-1)(x-t)(x+u)(x+tu)(x^2+tu), & q_{t,u} &= \frac{x dx^2}{y^2}. \end{aligned}$$

The order 4 rotation $\rho_1\sigma_1$ of $X_{t,u}$ persists on $\Xi_{t,u}$. Following R. Silhol [Si], we find a new parameter a , depending on t and u , so that the Riemann surface

$$\Xi_a : y^2 = x(x^2 - 1)(x - a)(x - 1/a)$$

is isomorphic to $\Xi_{t,u}$. Doing so simply requires a change of coordinates in x , namely

$$\Phi(x) = i\sqrt{tu} \frac{(x-1)}{(x+tu)}.$$

Then $\Phi(1) = 0$, $\Phi(-tu) = \infty$, and $\Phi(\pm i\sqrt{tu}) = \mp 1$. The images of t and u by Φ are

$$a = i\sqrt{\frac{u}{t}} \frac{(t-1)}{(u+1)} \quad \text{and} \quad \frac{1}{a} = i\sqrt{\frac{t}{u}} \frac{(1+u)}{(1-t)}.$$

Because $t > 1$ and $u > 0$, a lies on the positive imaginary axis and $1/a$ lies on the negative imaginary axis. The involution ρ becomes reflection across the imaginary axis. The images of 0 and ∞ by Φ are

$$\Phi(0) = \frac{i}{\sqrt{tu}} \quad \text{and} \quad \Phi(\infty) = \frac{\sqrt{tu}}{i},$$

so the image of $q_{t,u}$ on Ξ_a is a scalar multiple of

$$\left(x - \frac{i}{\sqrt{tu}}\right) \left(x - \frac{\sqrt{tu}}{i}\right) \frac{dx^2}{y^2} = \left(x^2 + i\left(\frac{tu-1}{\sqrt{tu}}\right)x + 1\right) \frac{dx^2}{y^2}$$

These calculations imply that, for each pair (t_0, u_0) , there is a one-parameter family of surfaces $(\Xi_{t,u}, q_{t,u})$ such that $\Xi_{t,u}$ is isomorphic to Ξ_{t_0, u_0} while $q_{t,u}$ and q_{t_0, u_0} represent different differentials on the abstract Riemann surface.

Now we apply the same analysis to the second family. This time we are moving from (X_s, ω_s) to (Σ_s, q_s) , as defined below:

$$\begin{aligned} X_s : y^2 &= x(x^2 + 1)(x - s)(x - \bar{s})(x + 1/s)(x + 1/\bar{s}), & \omega_s &= \frac{x dx}{y}; \\ \Sigma_s : y^2 &= (x^2 + 1)(x - s)(x - \bar{s})(x + 1/s)(x + 1/\bar{s}), & q_s &= \frac{x dx^2}{y^2}. \end{aligned}$$

We change coordinates in x using

$$\Psi(x) = i \left(\frac{x - s}{sx + 1} \right)$$

so that $\Psi(s) = 0$, $\Psi(-1/s) = \infty$, and $\Psi(\pm i) = \mp 1$. This time we get the curve $y^2 = x(x^2 - 1)(x - a)(x - 1/a)$, where

$$a = \Phi(\bar{s}) = \frac{2 \operatorname{Im} s}{1 + |s|^2} \quad \text{and} \quad \frac{1}{a} = \Phi\left(-\frac{1}{\bar{s}}\right) = \frac{1 + |s|^2}{2 \operatorname{Im} s}.$$

Here we have $0 < a < 1$ and $1/a > 1$; ρ' becomes inversion in the unit circle. The points 0 and ∞ on Σ_s become $\Phi(0) = -is$ and $\Phi(\infty) = i/s$. Again, we find just a one-parameter family of genus 2 Riemann surfaces, each carrying a one-parameter family of quadratic differentials corresponding to distinct surfaces X_s .

In [Si], it is shown that the full period matrix for any of the surfaces Ξ_a can be expressed in terms of a single parameter, thanks to the fourfold symmetry of the surface. This parameter is the ratio of $\int_{-1}^0 \varphi$ and $\int_0^{1/a} \varphi$, where $\varphi = \frac{dx}{y} - \frac{x dx}{y}$. This ratio is real precisely when a lies on the positive imaginary axis, as in our first family, and in these cases the period matrix of Ξ_a is purely imaginary.

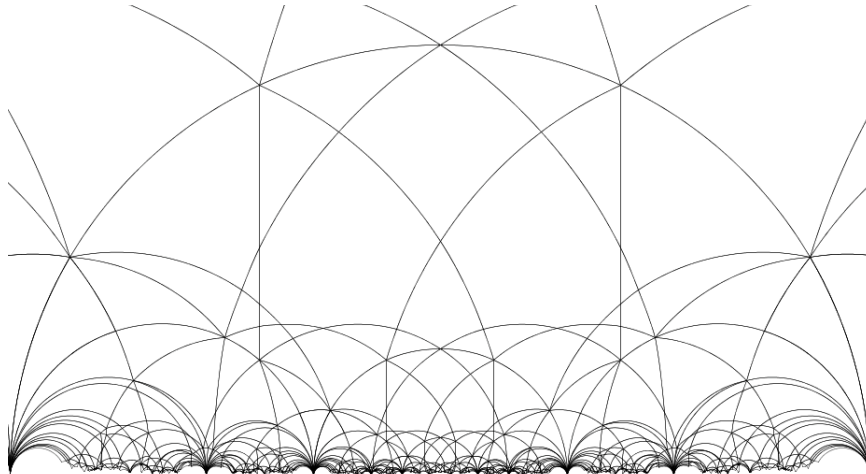


FIGURE 6. The iso-Delaunay tessellation of \mathbb{H} arising from $(X_{\text{AY}}, \omega_{\text{AY}})$

4. FINAL REMARKS

The involutions we have exhibited also act on the Teichmüller disk generated by $(X_{\text{AY}}, \omega_{\text{AY}})$, and their effects can be seen via the *iso-Delaunay tessellation* shown in Figure 6. The open regions in this picture correspond to combinatorial classes of Delaunay triangulations of surfaces in the $\text{SL}_2(\mathbb{R})$ -orbit of $(X_{\text{AY}}, \omega_{\text{AY}})$; points of the 1-skeleton correspond to surfaces with two or more Delaunay triangulations. Because Delaunay triangulations are not changed by any rotation of the surface, this picture can be drawn in the upper half-plane \mathbb{H} rather than its unit tangent bundle. Iso-Delaunay tessellations have been described previously in [Bo] and [Ve3]. We will not define them here, but simply illustrate how elements of the generalized Veech group $\Gamma \subset \text{GL}_2(\mathbb{R})$ of $(X_{\text{AY}}, \omega_{\text{AY}})$ may be seen to act on the tessellation in Figure 6. (The hyperelliptic involution, having derivative $-\text{id}$, acts trivially.)

Each element of Γ acts on \mathbb{H} by an isometry, preserving or reversing orientation according to the sign of its determinant. Figure 6 is symmetric with respect to the central axis (the imaginary axis in \mathbb{C}); both σ_1 and σ_2 yield elements of Γ that reflect \mathbb{H} across this axis. The hyperbolic element of Γ corresponding to ψ_{AY} fixes the points 0 and ∞ in $\partial\mathbb{H}$ and translates points along the imaginary axis by $z \mapsto z/\alpha^2$. A sequence of concentric circles is visible in the tessellation; these are related by ψ_{AY} , and one is the unit circle, so their radii are all powers of $1/\alpha^2 \approx 3.38$.

There are two kinds of distinguished points on the central axis: ones where two geodesics meet and ones where three geodesics meet. The latter are those whose corresponding surface is isometric to $(X_{\text{AY}}, \omega_{\text{AY}})$, while the former correspond to $(X'_{\text{AY}}, \omega'_{\text{AY}})$. The real structures ρ_1 and ρ_2 (resp. ρ'_1 and ρ'_2) yield an element of Γ that reflects \mathbb{H} across the unit circle (resp. across the circle $|z| = 1/\alpha$). The order 4 rotations of $(X_{\text{AY}}, \omega_{\text{AY}})$ and $(X'_{\text{AY}}, \omega'_{\text{AY}})$ are thus visible as the order 2 rotations of \mathbb{H} around these distinguished points.

If any other flat surface on the central axis had real structures, then its symmetries, too, would have to induce a reflection of \mathbb{H} that preserves the tessellation. No such point exists; therefore we have described all the surfaces within the orbit of $(X_{\text{AY}}, \omega_{\text{AY}})$ under the geodesic flow that demonstrate additional symmetries.

REFERENCES

- [Ar] Pierre Arnoux. Un exemple de semi-conjugaison entre un échange d'intervalles et une translation sur le tore. *Bull. Soc. Math. France* **116**(1988), 489–500.
- [AY] Pierre Arnoux and Jean-Christophe Yoccoz. Construction de difféomorphismes pseudo-Anosov. *C. R. Acad. Sc. Paris Sr. I Math.* **292**(1981), 75–78.
- [BS] Alexander I. Bobenko and Boris A. Springborn. A discrete Laplace–Beltrami operator for simplicial surfaces. *Discrete Comput. Geom.* **38**(2007), 740–756.
- [Bo] Joshua P. Bowman. Teichmüller geodesics, Delaunay triangulations, and Veech groups. *Proceedings of the International Workshop on Teichmüller theory and moduli problems*, to appear.
- [EG] Clifford J. Earle and Frederick P. Gardiner. Teichmüller disks and Veech’s \mathcal{F} -structures. *Contemp. Math.* **201**(1997), 165–189.
- [EO] Alex Eskin and Andrei Okounkov. Asymptotics of numbers of branched coverings of a torus and volumes of moduli spaces of holomorphic differentials. *Invent. Math.* **145**(2001), 59–103.
- [HS] Frank Herrlich and Gabriela Schmithüsen. On the boundary of Teichmüller disks in Teichmüller and Schottky space. In A. Papadopoulos, editor, *Handbook of Teichmüller Theory*. European Mathematical Society, 2007.
- [HM] John H. Hubbard and Howard Masur. Quadratic differentials and foliations. *Acta Math.* **142**(1979), 221–274.
- [HL] Pascal Hubert and Erwan Laneeau. Veech groups without parabolic elements. *Duke Math. J.* **133**(2006), 335–346.
- [HLM] Pascal Hubert, Erwan Laneeau, and Martin Möller. The Arnoux–Yoccoz Teichmüller disc. *Geom. and Func. Anal.*, to appear.
- [La] Erwan Laneeau. Hyperelliptic components of the moduli spaces of quadratic differentials with prescribed singularities. *Comm. Math. Helv.* **79**(2004), 471–501.
- [LS] Samuel Lelièvre and Robert Silhol. Multi-geodesic tessellations, fractional Dehn twists and uniformization of algebraic curves. Preprint, available online at <http://arxiv.org/pdf/math.GT/0702374v1>.
- [MS] Howard Masur and John Smillie. Hausdorff dimension of sets of nonergodic measured foliations. *Ann. Math.* **134**(1991), 455–543.
- [Mc] Curtis T. McMullen. Dynamics of $SL_2(\mathbb{R})$ over moduli space in genus two. *Ann. Math. (2)* **165**(2007), 397–456.
- [Ri] Igor Rivin. Euclidean structures on simplicial surfaces and hyperbolic volume. *Ann. Math.* **139**(1994), 553–580.
- [Sch] Gabriela Schmithüsen. An algorithm for finding the Veech group of an origami. *Exp. Math.* **13**(2000), 459–472.
- [Si] Robert Silhol. Genus 2 translation surfaces with an order 4 automorphism. *Contemp. Math.* **397**(2006), 207–213.
- [Va] Sergey Vasilyev. Genus two Veech surfaces arising from general quadratic differentials. Preprint, available online at <http://arxiv.org/pdf/math.GT/0504180>.
- [Ve1] William A. Veech. Teichmüller curves in moduli space, Eisenstein series, and an application to triangular billiards. *Inv. Math.* **97**(1989), 553–583.
- [Ve2] William A. Veech. Delaunay partitions. *Topology* **36**(1997), 1–28.
- [Ve3] William A. Veech. Bicuspid F -structures and Hecke groups. Preprint.
- [Zo] Anton Zorich. Square tiled surfaces and Teichmüller volumes of the moduli spaces of abelian differentials. In *Rigidity in dynamics and geometry (Cambridge, 2000)*, pages 459–471. Springer, Berlin, 2002.

DEPARTMENT OF MATHEMATICS, CORNELL UNIVERSITY, ITHACA, NY 14853